

SEISMIC BEHAVIOUR OF CONCRETE FRAMES: EXPERIMENTAL AND ANALYTICAL VERIFICATION OF EUROCODE 8 DESIGN RULES

Fabio BIONDINI

Giandomenico TONIOLO

Department of Civil Engineering, Technical University of Milan, Italy

Keywords: precast structures, seismic design, Eurocode 8, dynamic analysis, pseudodynamic tests.

1. INTRODUCTION

The works of revision of Eurocode 8 for its conversion from provisional ENV status to final EN status are finished and the new text is going to formal vote. Significant improvements of design provisions for precast structures have been introduced in the new text. In fact the old Annex B of ENV 1998-1-3:1994 was mainly referred to large-panel wall systems and shaped on the basis of the low ductility of these systems. It recited: "ductility classes medium M and low L will be normally considered" for precast construction, while for "ductility class high H ... an additional special study shall be undertaken". And this clashed in our ears, since we know very well that precast columns may have exactly the same ductility than cast-in-situ columns.

Furthermore, in the very beginning of the annex, within the precast structural systems the notorious ill-famed "pendulum system" was listed as if it was typical of precast systems. Together with the attached note, this definition suggested that "single storey industrial buildings with doubly hinged beams" should be considered inverted pendulums. Since the behaviour factor of pendulum systems is 2,5 times lower than for frame systems, this would mean that one should assume seismic forces 2,5 times larger than in national regulations and no precast industrial buildings would be built any longer. The situation was characterised by heavy unjustified preconceptions against precast constructions.

In the last draft of prEN 1998-1 (see [01]), no unjustified inequalities between precast and cast-in-situ construction are present. The "pendulum systems" have been deleted from the list of precast types of structures. Any requirement for special study has been deleted too and ductility properties have been equalised to those of cast-in-situ structures. This applies under the necessary condition that connections between precast elements are located out of the critical zones, or overdimensioned with a capacity design or provided with energy dissipation capacity. Finally one storey industrial buildings, where the column tops are connected along both the main directions by hinges, may have the same behaviour factor of frame systems.

1.1. Ductility of r.c. columns

For elements in flexure such as beams and columns belonging to frame systems, the basic ductility resource is measured by the ratio $\mu_\varphi = \chi_u / \chi_y$ between the ultimate curvature of the section and the curvature at the yield limit.

Calling $\chi_p = \chi_u - \chi_y$ the plastic curvature, the ductility ratio can be written as:

$$\mu_\varphi = 1 + \frac{\chi_p}{\chi_y} = 1 + \mu_p \quad (1)$$

If expressed in terms of displacement, i.e. the interstorey drift of a single column with the end sections fixed to the beams, the value of the corresponding ductility ratio $\mu_\delta = \delta_u / \delta_y$ can be computed from the elastic displacement at the yield limit $\delta_y \cong \chi_y h^2 / 6$ and the displacement corresponding to the plastic curvature $\delta_p \cong \varphi_p h = \chi_p h_p h$ (see Fig. 1a) obtaining, with $\delta_u = \delta_y + \delta_p$:

$$\mu_\delta = 1 + \frac{\delta_p}{\delta_y} = 1 + 6 \frac{h_p}{h} \mu_p \quad (2)$$

Provided an overstrength ratio $(f_t / f_y) \geq 1.15$ of the steel, with the other contributions ensure plastic zones with a length around $h_p \cong 0.083h$, the displacement ductility of the element remains lower than the curvature ductility of the section, as given by the following equation (with $\mu_p = \mu_\varphi - 1$)

$$\mu_\delta \cong 1 + 0.5\mu_p = \frac{1}{2}(1 + \mu_\varphi) \quad (3)$$

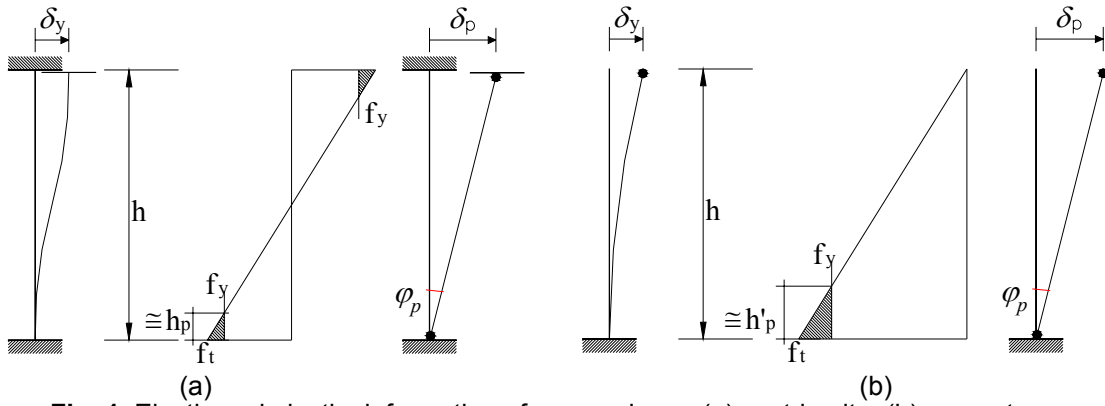


Fig. 1. Elastic and plastic deformation of a r.c. column: (a) cast-in-situ; (b) precast.

1.2.Ductility of r.c. frames

The link between the local ductility and the global ductility of the structure, which gives its potential capacity of energy dissipation under earthquake action, is based on the ultimate failure mechanism. The plastic hinge distribution at this ultimate condition establishes the geometrical relation, which can lead to much different results, as shown in the well known sketches of Fig. 2. Fig. 2a indicates the elastic deformation of the multistorey frame at the yield limit, where the global displacement is of the order of $d_y \cong n\delta_y$. Fig. 2b shows the good failure mechanism ensured by the capacity design rule of weak beams in strong column. Here again the global displacement is $d_p \cong n\delta_p$ and the ductility ratio remains of the same order as the element ductility:

$$\mu_\Delta = \frac{d_y + d_p}{d_y} \cong \frac{n\delta_y + n\delta_p}{n\delta_y} = \mu_\delta \tag{4}$$

Fig. 2c shows the bad weak-storey mechanism where, with $d_p = \delta_p$, the global ductility ratio becomes:

$$\mu_\Delta = \frac{d_y + d_p}{d_y} \cong \frac{n\delta_y + \delta_p}{n\delta_y} = 1 + \frac{1}{n}(\mu_\delta - 1) \tag{5}$$

For the four-storey frame of Fig. 2, with an element ductility ratio of $\mu_\delta = 5$, a global ductility of only $\mu_\Delta = 2$ would derive.

For the one-storey frame of Fig. 3, with $n=1$ the global ductility ratio is always equal to the element ductility ratio ($\mu_\delta = \mu_\Delta$) independently from the position of the upper plastic hinges (see Fig. 2b-c). In this case the capacity design rule of weak beam in strong column is not needed.

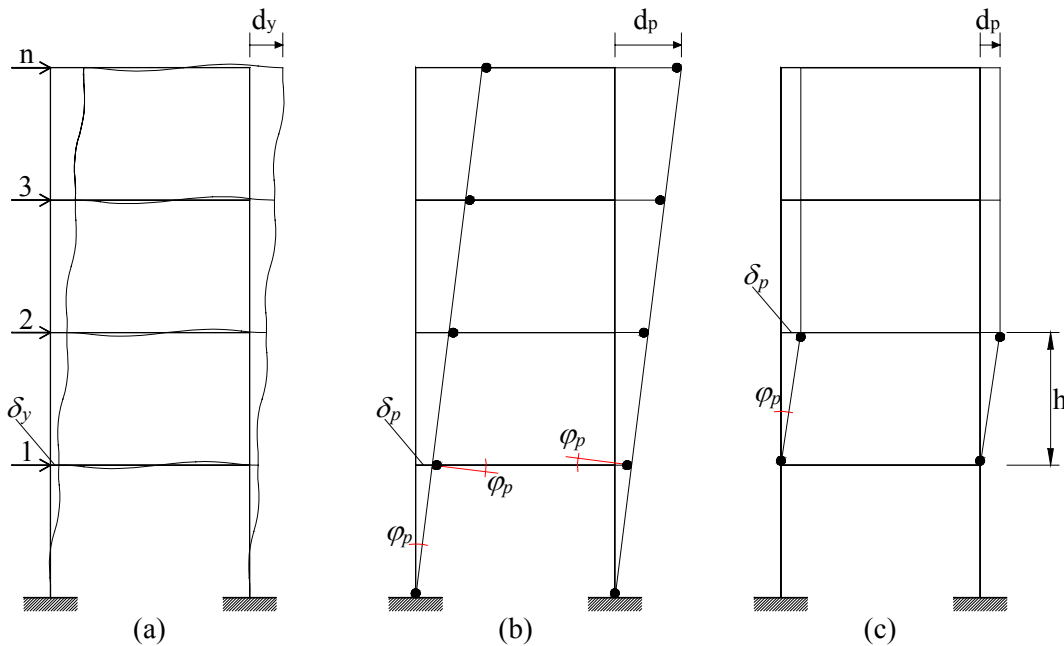


Fig. 2. Failure mechanisms of a multistorey frame.

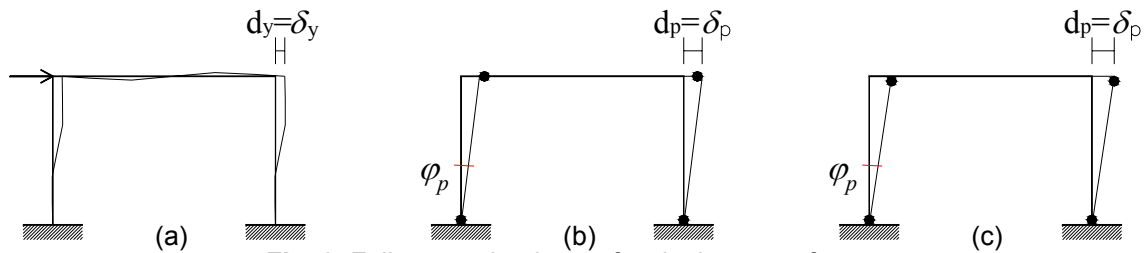


Fig. 3. Failure mechanisms of a single-storey frame.

1.3. Precast hinged frames

If the one-storey frame is built with a precast beam hinged at the top of the columns, the displacement ductility can be computed from the elastic $\delta_y \cong \chi_y h^2 / 3$ and plastic $\delta_p \cong \chi_p h_p' h$ contributions (see Fig. 1b), obtaining $\mu_\delta = 1 + 3(h_p' / h)\mu_p = \mu_\Delta$ which leads, for the same steel of Fig. 1a with $h_p' \cong 2h$ and $\mu_p = \mu_\phi - 1$, to the same relation between the curvature ductility ratio and the displacement ductility ratio $\mu_\delta = (1 + \mu_\phi) / 2 = \mu_\Delta$. In terms of pure ductility the behaviour of a precast hinged frame may be equivalent to the behaviour of a cast-in-situ monolithic frame.

The inequality between precast and cast-in-situ r.c. frames stated by the old ENV Eurocode 8 results from a wrong reading of the fundamental requirement for the structural ductility necessary for energy dissipation: "An overall ductile behaviour is ensured if the ductility demand is spread over a large number of elements and locations in the structure". In fact the cast-in-situ frame of Fig. 4a has four dissipating zones, the double than the precast frame of Fig. 4b. But, for the same horizontal force, the precast upper-hinged columns will have double bending moments, which will lead to a double proportioning. In such a way the same amount of energy dissipated in the four critical zones of the monolithic frame could be dissipated in the two larger critical zones of the hinged frame ($2U = 4u$). The requirement of Eurocode 8 is now better worded: "An overall ductile behaviour is ensured if ductility demand involves globally a large volume of the structure spread to different elements and location of all its storeys." In fact it is not the number but the global volume involved in dissipation that gives the total amount of energy dissipated by the structure and this is valid under the condition that early collapses due to soft storey mechanism don't occur, condition verified, for multistorey frames, by the proper capacity design with the rule of weak beams in strong columns.

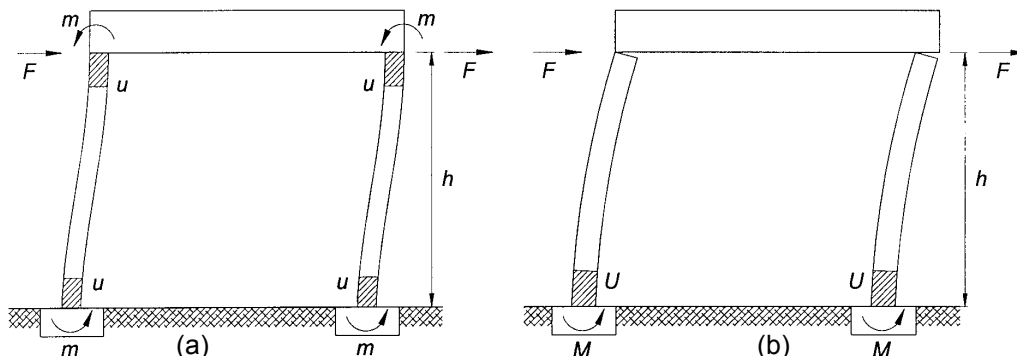


Fig. 4. Energy dissipated by the frames: (a) monolithic arrangement; (b) hinged arrangement.

1.4 Force reducing factor

In the scope of the equivalent force method regulated by Eurocode 8 [01], the acceleration forces can be reduced by the behaviour factor q , with respect to the pure elastic response, to account for structural ductility μ_Δ . The relation between q and μ_Δ depends on the first natural vibration period T_1 of the structures. For the longer vibration periods of flexible structures, the criterion of "equal displacement" can be assumed, which leads to $q = \mu_\Delta$.

With reference again to the elements of frame structures such as columns and beams, Eurocode 8 gives the rules for steel properties and reinforcement detailing of critical zones necessary to achieve a certain value of ductility ratio. In high ductility class the order of this value is $\mu_\phi \cong 9$. From the above value and from the capacity design rule which ensures elements with strong shear and weak moment strength, a displacement ductility ratio of about $\mu_\delta \cong (1 + \mu_\phi) / 2 = 5.0$ comes out for the elements. Finally the capacity design rule of weak beam in strong column ensures, also for multistorey frames, a global ductility ratio of the same order $\mu_\Delta \cong \mu_\delta = q = 5.0$.

But this value doesn't take into account the rough reliability of the model assumed in Eurocode 8, with its elastic response spectra, to represent the seismic action. To cover this scanty compatibility of the design model with respect to the features of real earthquakes (see [03]) the behaviour factor shall be decreased to $q = 4.5$ which is the basic value given by the new Eurocode 8 to frame systems, not inclusive of the overstrength factor α_u / α_1 due to structural redundancy.

2. ANALYTICAL APPROACH

2.1. Verification of behaviour factors

Eurocode 8 gives a scale of q -factors related to the different types of structures, with their potential capacity of energy dissipation conventionally evaluated on the base of the ultimate failure mechanism. At present such q -values are defined more or less on the base of empirical choices, not supported by a rigorous calculation of sufficient reliability. The experience of different seismic countries has contributed to this definition, through compromises reached during the works of the competent European committee. This empirical procedure may lead to unjustified inequalities between different materials and structures.

In order to try a more reliable definition of the behaviour factors, a rigorous analytical approach shall be applied. But the problem is not simple, since seismic event has the characteristics of a multivariable random process which cannot be reduced to a deterministic "limit state" problem of only intensity. The duration of the violent phase, the frequency content, the peak accelerations and their spectral distribution are only some of the distinctive parameters of seismic action which impact the corresponding structural characteristics of strength and ductility, of cyclic decay and of natural vibration frequencies. The random combination of the ground motion phases leads to more or less heavy effects on the specific structure and this depends on the location of the major shocks with respect to the phase of the contemporary oscillation of the structure (in favour or in opposition of phase).

The dependence of the structural behaviour from the specific ground motion can be considered with an incremental collapse dynamic analysis, which starts from a specific accelerogram, increasing its peak acceleration on a step by step procedure, repeated until failure is reached. But one response is not sufficient to cover the large random variability of the seismic event. An exhaustive response requires a full probabilistic Monte Carlo approach based on a large set of recorded or artificial accelerograms covering the range of possible expected ground motions.

2.2. Non linear dynamic analysis

The dynamic non-linear analysis of the one-storey frames under examination is based on the single degree of freedom motion equation:

$$m \ddot{d}(t) + c \dot{d}(t) + k(d)d(t) = -m a(t) \quad (6)$$

where m is the vibrating mass, c is the viscous damping coefficient (assumed equal to 5% of the critical one), $k(d)$ is the degrading elastoplastic stiffness and $a(t)$ is the ground acceleration. The top displacement d of the structure is an unknown function of the time t . The static term, corresponding to the shear force $V(d)$ of the columns, is directly given as:

$$k(d)d(t) = V(d) = F(d) - \frac{N_{ad}}{h} d(t) \quad (7)$$

where the last term represents the second order effect of the vertical load N_{ad} acting on the columns and $F(d)$ is read on the proper force-displacement model as a function of the preceding load history.

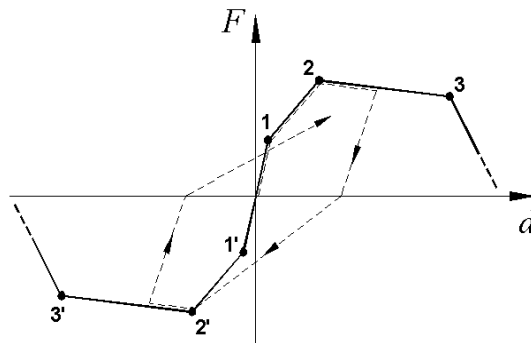


Fig. 5. Degrading stiffness model.

The F - d function of the degrading elastoplastic stiffness has been derived from Takeda model, completed with a decreasing branch as introduced by Priestley et al. [12] in order to represent the ultimate phase of failure. Fig. 5 shows the envelope curve of hysteretic cycles, where the limit points of the model correspond respectively to the first cracking of the critical section, to the yielding of reinforcement and to the compressive failure of concrete core (for more details see [02]).

The quoted model refers to a flexural mode of failure. This mode is ensured by the slenderness of the columns. In addition it is assumed that a proper capacity design ensures the full efficiency of the connections, so that the collapse of the overall structure comes from the failure of the critical sections of the columns. Their strength and ductility, as represented by the F - d model, give the seismic capacity of the structure.

Based on this model, the structural response to given ground motions is computed for increasing values of peak ground acceleration a_g starting from $\alpha_g = a_g/g = 0.30$ with increments $\Delta\alpha_g = 0.05$ up to collapse. The collapse itself is pointed out by the loss of the vibratory equilibrium, shown by an unlimited increase of the displacement. The last value of peak ground acceleration α_{gmax} before collapse is assumed to represent the "experimental" seismic capacity of the structure.

2.3. Check of the design capacity

The experimental capacity $\alpha_{g\max}$ has been compared to the theoretical one given by the design rules of Eurocode $\bar{\alpha}_g = [q/(2.5\eta)](F_d/W)$, where $\eta = \eta(T) \geq 0.08q$ is the decreasing function $\eta = T_c/T$ for $T_c \leq T \leq T_D$ and $\eta = T_c T_D/T^2$ for $T_D < T$ (in the following applications a subsoil type 1A is assumed, with $T_c=0.4$ sec and $T_D=2.0$ sec), and F_d is the ultimate limit value of the seismic force related to the resistant moments M_{rd} of the critical sections: $F_d = 2M_{rd}/h$ for the cast-in-situ frame and $F_d = M_{rd}/h$ for the precast frame. The seismic performance of the structures are then described in terms of the overstrength ratio between experimental and theoretical seismic capacities $\kappa = \alpha_{g\max}/\bar{\alpha}_g$ of which a value equal 1 represents the perfect correspondence between design theory and "test" results.

An application of the procedure is shown with reference to the frames of Fig. 6. Structural data can be found in [02]. With a total effective gravity load $2W = 2 \times 187.2$ kN the first natural vibration periods are $T=1.87$ sec for type (a), $T=2.12$ sec for type (b). And with the resistant moments $M_{rd}=91.07$ kNm and $M_{rd}=17.56$ kNm, the theoretical design capacities becomes respectively $\bar{\alpha}_g = 0.162q$ for the cast-in-situ frame and $\bar{\alpha}_g = 0.158q$ for the precast frame. With the value $q=4.5$ given by Eurocode 8 to r.c. frame systems, these capacities become $\bar{\alpha}_g = 0.729$ for the cast-in-situ frame and $\bar{\alpha}_g = 0.711$ for the precast frame.

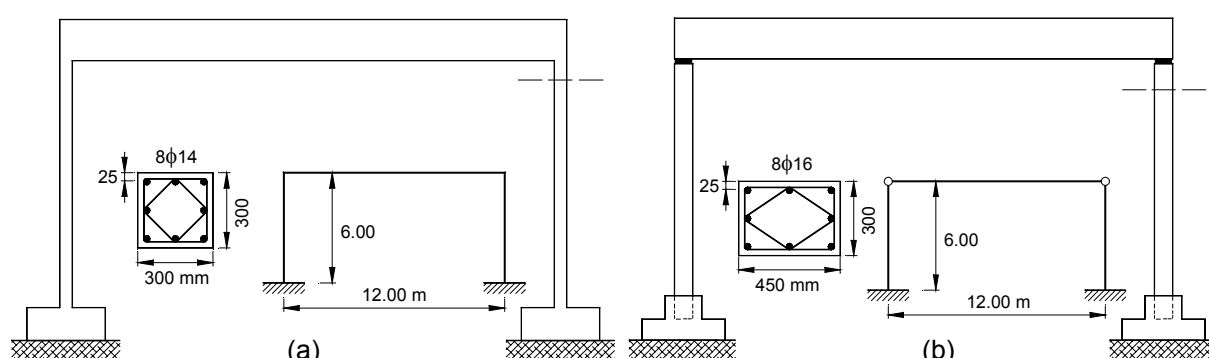


Fig. 6. Scheme of the frame: (a) monolithic arrangement; (b) hinged arrangement.

2.4. Use of recorded accelerograms

At a first step of the statistical investigation, the only randomness of the seismic action is considered, assuming for the material properties their 5% characteristic value and using recorded accelerograms.

Recorded accelerograms of earthquakes are available in large number in the database of specialised institutions (see for example [17]). Fig. 7 shows one of these accelerograms together with the corresponding elastic response spectrum superimposed to Eurocode 8 spectrum for subsoil type 1A.

The main drawbacks of recorded accelerograms are the following:

- they are in general poor of frequencies and may lead, for the same value of the peak acceleration, to much different responses of the structures;
- they have a rough compatibility with the response spectra of the code, so to introduce additional uncertainties in the comparison with the design rules;
- they have a scarce homogeneity between them so to form sets not well compatible with a rigorous statistical elaboration of the results;
- they are of insufficient numerosness for the computation of stabilised statistical parameters of the response.

On the other hand they reproduce exactly the nature of the real earthquakes.

A set 65 accelerograms having a reasonable minimum compliance measured in terms of variance over the frequency range with the response spectrum of the Eurocode have been used for a statistical investigation to calibrate the behaviour factors. The results of this investigation are summarised in Fig. 8, which shows the density distributions of the overstrength ratio computed with $q=4.5$. A large scatter

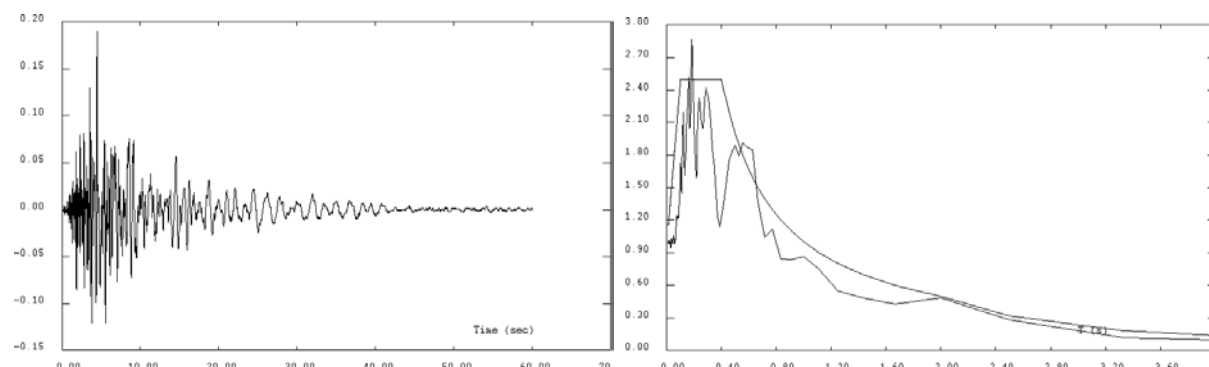


Fig. 7. Accelerogram $a(t)/g$ and elastic response spectrum $S(T)/a_{\max}$: Mammoth Lakes, May 25 1980, Gilroy.

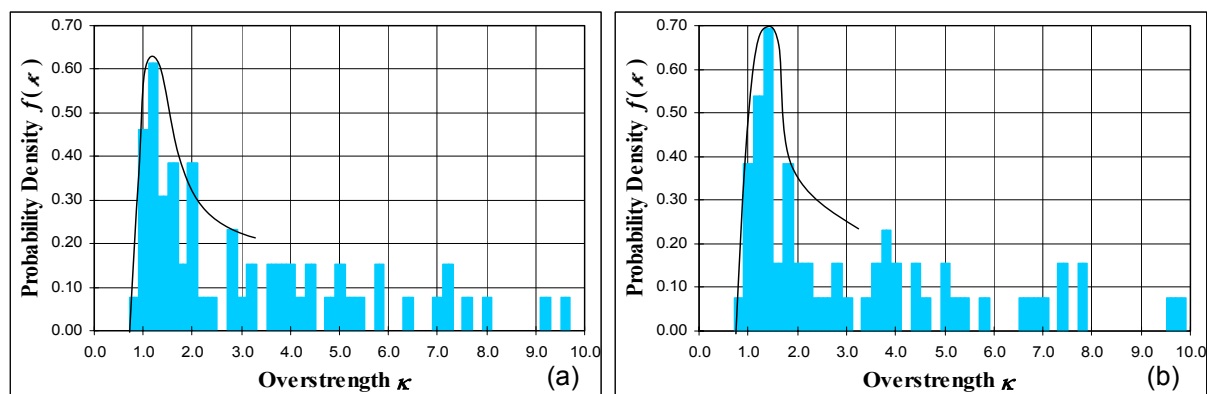


Fig. 8. Density distribution of the overstrength: (a) monolithic and (b) hinged frames.

of the data can be noticed, mainly due to the limited compatibility of recorded ground motions with the response model assumed in Eurocode 8. A direct comparison of these diagrams shows the very good correspondence between the seismic performance of the two types of structures. The 5% fractile correspond approximately to the value $\kappa \approx 1$, which confirms the correctness of the q -value 4.5 too. However, the sample seems too small for a reliable statistical evaluation.

2.5. Use of artificial accelerograms

In order to overcome the drawbacks related to the use of recorded accelerograms, artificial accelerograms can be generated so to match with good compatibility the response spectrum of the code. Fig. 9 shows one of these accelerograms generated with the program SIMQKE [16] together with their elastic response spectra. The main features of artificial accelerograms are the following:

- they are rich of frequencies with a more defined response of the structure for a given value of the peak ground acceleration;
 - they can be generated so to match with good precision the response spectra of the code and allow a reliable comparative verification of its design rules;
 - they may have homogeneous features, through a wide random variation of the shape parameters, so to permit a rigorous statistical elaboration of the results;
 - they may give sets of numerosness large at will following the requirements of the statistical processes.
- On the other hand they are not fully realistic with respect to the nature of actual earthquakes.

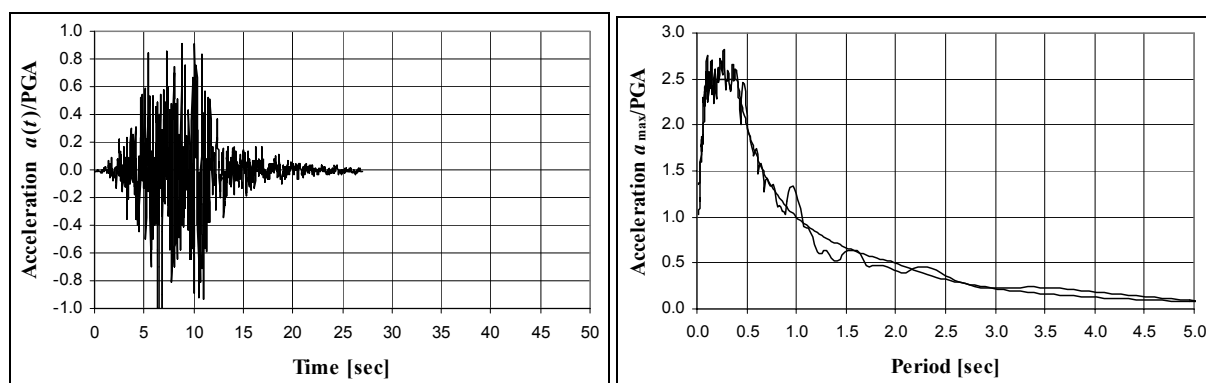


Fig. 9. Artificial accelerogram and its response spectrum.

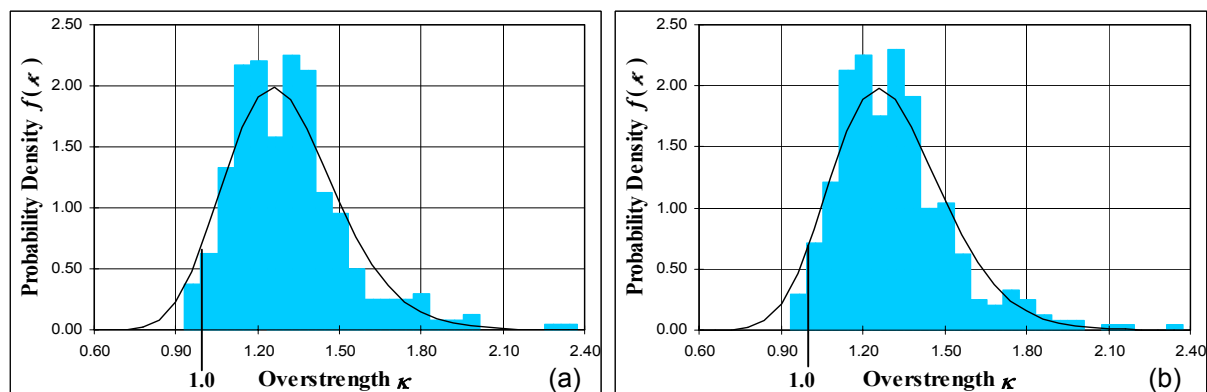


Fig. 10. Density distribution of the overstrength: (a) monolithic and (b) hinged frames.

At a second step of the statistical investigation, such artificial accelerograms are used, again with the only randomness of the seismic action. The density distributions of the overstrength ratio computed with $q=5$ for a sample of 400 artificial accelerograms are shown in Fig. 10. A direct comparison of these diagrams confirms the very good correspondence between the seismic performance of the two types of structures. A lognormal regression of the data leads to a 5% fractile which corresponds in both cases to the value $\kappa \cong 1$. This last result indicates that the q -value 4.5 given by Eurocode 8 may also cover the uncertainty of the model of the seismic action with respect to the large variability of the real earthquakes and the limited amount of information about them.

2.6. Randomness of material properties

At a third step, in order to achieve a full probabilistic verification of the seismic performance of the frames, the randomness of the material strengths is also introduced. To this aim, both concrete and steel strengths are assumed as random variables with lognormal distributions defined by the characteristic values (5% fractile) and the standard deviations: $f_{ck} = 40$ MPa and $s = 5$ MPa for concrete, $f_{yk} = 500$ MPa and $s = 30$ MPa for steel.

Fig. 11 shows the density distributions of the overstrength ratio κ computed again with $q=5$ and obtained from a Monte Carlo simulation carried out for a sample of 1000 sets of random quantities (accelerogram and material properties). The comparison between the behaviour of the two frames is again very good. Moreover, since material strengths vary around mean values sensibly higher than the characteristic value, the probability distributions move right and the 5% fractile increases in both cases to the value $\kappa \cong 1.27$. This additional margin may also covers the approximations of the analytical model used in the dynamic analyses.

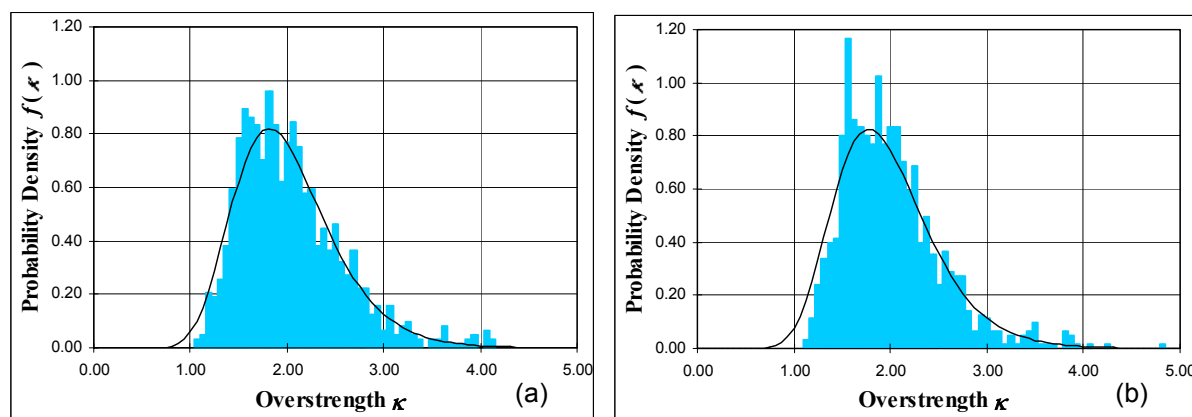


Fig.11. Density distribution of the overstrength: (a) monolithic and (b) hinged frames.

The analytical probabilistic approach shows that cast-in-situ and precast concrete frames have the same seismic capacity and that the value 4.5 given by Eurocode 8 to the behaviour factor for these frames have a full reliability. It is to be noted that the capacity of the frames for $q=4.5$ is very high ($\bar{\alpha}_g$ about 0.72), the double of what required in Italy for seismic zones of first category. This is due to the high values of their natural vibration periods (about 2 seconds), which lead to a reduced response to the ground motion. Therefore, these type of frames have a large margin of safety with respect to seismic collapse. They find their dimensioning from the non-seismic conditions (such as the wind pressure) and the seismic serviceability limit state referred to the storey drift.

3. EXPERIMENTAL ASSESSMENT

3.1. Precast prototype

The pseudodynamic tests described below has been performed, within the Ecoleader Programme, at ELSA European Laboratory for Structural Assessment of Ispra (Italy). Two structural prototypes have been designed, both consisting of six columns connected by two lines of beams and an interposed slab. The connections between columns and beams are made with monolithic joints for the cast-in-situ arrangement and with hinged joints for the precast one. The 5th and 6th September 2002 the pseudodynamic test on the precast structure has been performed.

Fig. 12 shows the deck plan and the longitudinal section (parallel to the applied seismic action). For the foundations, six pocket blocks have been made, anchored to the base deck of the testing plant. The columns have been inserted in the pockets and fixed with no-shrinkage mortar, leaving two lateral rooms necessary to introduce the instrumentation down to the column bottoms. The overall dimensions of the prototype are given in the quoted figure. The columns have cross sizes 300x450 mm and are reinforced with 8 bars $\phi 16$ and stirrups $\phi 6$ spaced by 50 mm in the lower part (which includes the critical zone of the flexural strength) and by 150 mm in the upper part. Steel class B500 has been used. In the lower part, threaded rods $\phi 10$ have been inserted transversally to fix the instruments. Concrete strength class is C40/50. For more detailed information see [07].

3.2. Testing plant

The prototype to be submitted to pseudodynamic test has been proportioned with the aim to reproduce possible real dimensions of a precast structure. Naturally, for economy reasons, all dimensions not affecting the structural behaviour under consideration have been reduced, replacing the missing weights by means of proper vertical jacks. The inertia forces are numerically simulated in the model governing the pseudodynamic procedure, together with the related second order effects. The two principal horizontal jacks have been connected with spherical joints to the deck, close to the midspan of the first bay. They were controlled in tandem with a master-slave system so to obtain a uniform translation of the deck. The displacements to be applied were controlled by means of digital transducers. Fig. 13 shows the scheme of the testing plant.

The data recording system has been extended to the “active” quantities (such as the applied displacements and the corresponding forces) and to the “passive” quantities (such as the local strains read by the instrumentation distributed over the structure).

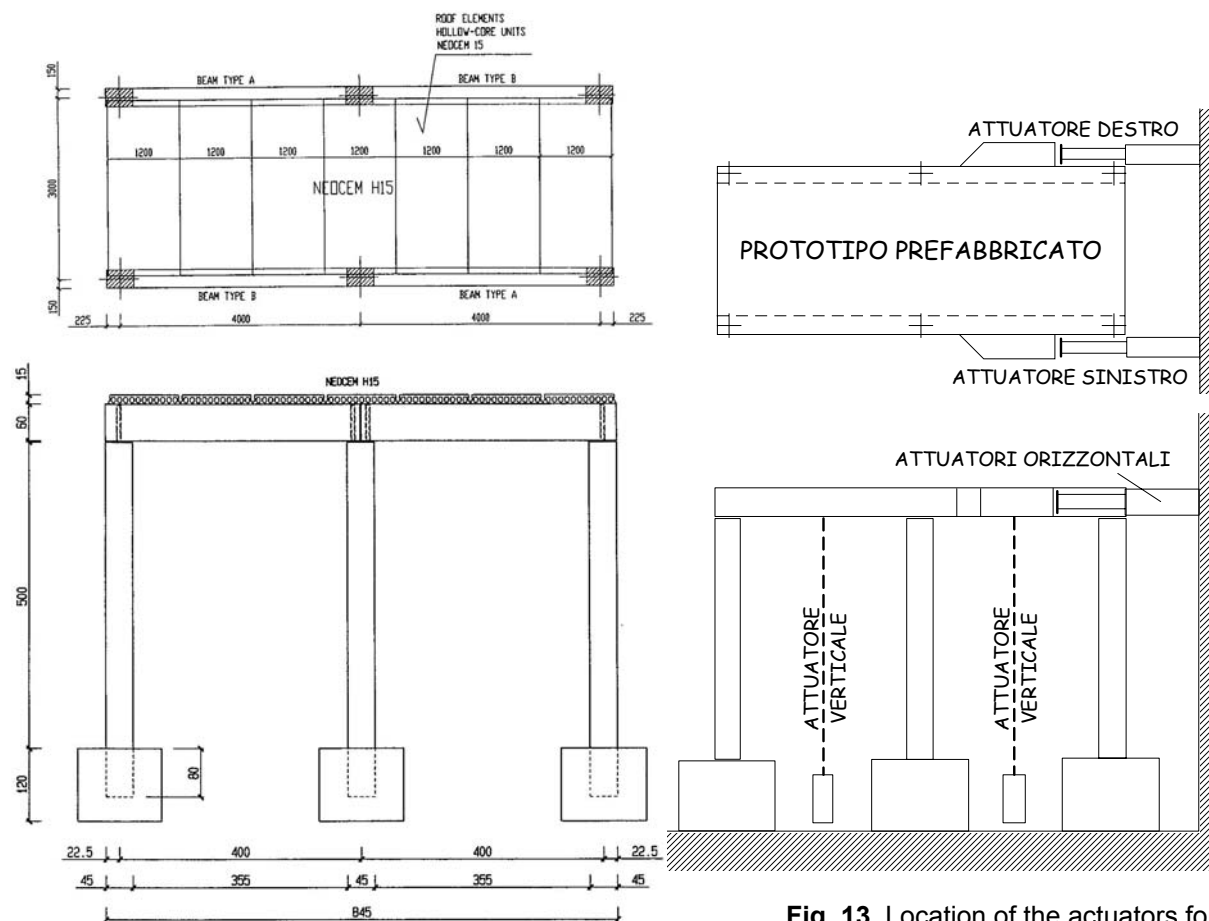


Fig. 12. Plant and longitudinal view of the precast prototype.

Fig. 13. Location of the actuators for the pseudodynamic test.

3.3. Testing programme

The seismic action for the pseudodynamic test has been simulated by an artificial accelerogram automatically generated so to be compatible with the response spectrum given by Eurocode 8 for a subsoil type 1B (very dense sand or gravel). Fig. 14 shows this accelerogram together with the corresponding response spectrum superimposed to the Eurocode 8 spectrum. Through previous non-linear dynamic analyses, elaborated using a suitable model of degrading stiffness of the columns, a theoretical collapse limit equal to $\alpha_g = 1,18$ has been quantified (versus a value of $\alpha_g = 1,08$ obtained from Eurocode 8 rules).

Taking into account the expected collapse limit, three load steps have been scheduled, respectively at 1/3, 2/3 and 3/3 of EC8 ultimate strength. More in details:

- 1st step at $\alpha_g = 0,36$

could represent the serviceability limit state for the verification of the storey drift and should leave the structure in elastic phase, with small cracks closed back at the unloading, without relevant damaging (actually this intensity correspond to about what given in Italy for the verification of the ultimate collapse limit for a 1st category zone.);

- 2nd step at $\alpha_g = 0,72$

could represent the ultimate limit state for the verification of the structural strength and should take the structure into the plastic phase with relevant permanent cracking and residual deformations at the unloading; this was intended as the last significant step, in view of the large damaging, but sufficiently far from the expected collapse of the prototype to ensure a complete execution of the test without unforeseen obstacles;

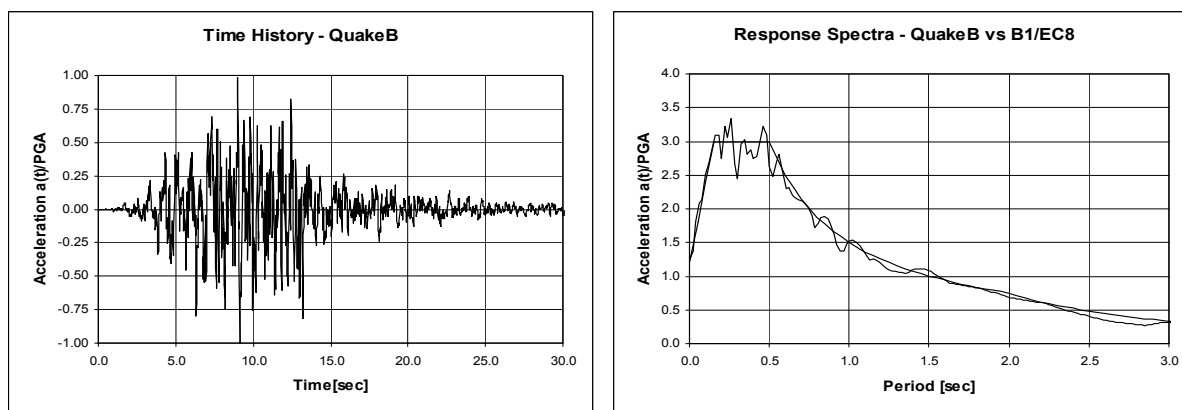


Fig. 14. Time histories and response spectrum of the used artificial accelerogram.

- 3rd step at $\alpha_g = 1.08$

should not be a significant reference for the verification of seismic behaviour of the structure, because of the damaging previously produced; but it represent an interesting opportunity to take the prototype to the extreme conditions and collect further useful information for the subsequent theoretical investigations.

For the interpretation of the results, some additional data have to be given. The ultimate resistant force, computed with the nominal properties of materials and taking into account the ultimate damaging of the structure, is $E_{rd} = 210$ kN. If the actual material properties are referred to without damaging, the strength rises to $E_{rd} \approx 265$ kN. Finally, if the hardening of steel is accounted for, as measured with the tensile tests on the reinforcing bars, the strength attains $E_{rd} \approx 320$ kN. This could be the reaction force reached at the first cycles of the dynamic test, when the structural decay has just begun. Furtheron the displacement at the first full yielding limit of the reinforcement, evaluated with the traslatory stiffness at the level of the resistant moment of the non damaged structure, is $d''_y \approx 110$ mm, while the outer tensioned bars start yielding at $d'_y \approx 85$ mm.

3.4. Experimental results

From the large set of data recorded during the test, this paper reproduce only the vibration curves of the upper deck and the corresponding force-displacement diagrams (see Fig. 15).

The diagrams of the first step at $\alpha_g = 0.36$ show maximum displacements between +90 and -100 mm, about the limit of the first yielding. They show again one only cycle with sensible hysteresis and a vibratory behaviour substantially elastic, stabilised along the reduced stiffness of the cracked columns and without any residual deformation. The cracks, observed at the maximum displacements and measured in terms of few tenths of millimeter, closed again at unloading. Then it can be assumed that the structure kept its full strength capacity.

The diagrams at the second step at $\alpha_g = 0.72$ show maximum displacements between +180 and -220 mm, far beyond the limit of full yielding of the reinforcement, with several cycles of large hysteresis, forces raised to +300 and -320 kN corresponding to the ultimate strength of the sections with hardened reinforcement and with cracks up to some millimeter at the maximum displacements, only partially closed back at unloading. The residual displacement of about -25 mm indicates the irreversible effects of a certain structural damage. But on the whole, except for some spallings at the top edges of the columns, due to the concentrated pressure of the beams under the maximum deflection of the columns, the structure didn't show damages decisive with respect to its strength resources.

At the level $\alpha_g = 1.08$ of the third step, maximum displacements between 400 and 450 mm were expected at the limit of the maximum stroke of the jack pistons. The possibility of full completing of the test was not sure. Actually, after the first violent shocks, due to the residual displacement of the preceding loading step, the amplitude of the motion took the jacks to the end of stroke and the test had to be stopped. The only information which can be taken is that, for the maximum displacement of 400 mm, the cover of the critical zones of the columns was still entire and the reaction forces at the level of 320 kN without any incipient decay. The ultimate collapse limit was still far. This situation is reproduced in the picture of Fig. 16.

3.5. Calibration of the analytical model

The results of the pseudodynamic test allowed to assess the analytical model used in the dynamic analysis. Fig. 17 reproduces the computed vibration curves superimposed to the experimental curves. In the analytical model the strength parameters have been introduced with their actual values as tested in samples of the materials. For the two higher levels of seismic action, the point 1 of the model of Fig. 5 has been omitted, since the structure had already overcome the first cracking limit. A value $c = 0$ of the viscous damping has been assumed, consistently to the physical behaviour of the prototype under the pseudodynamic test and to its control algorithm.

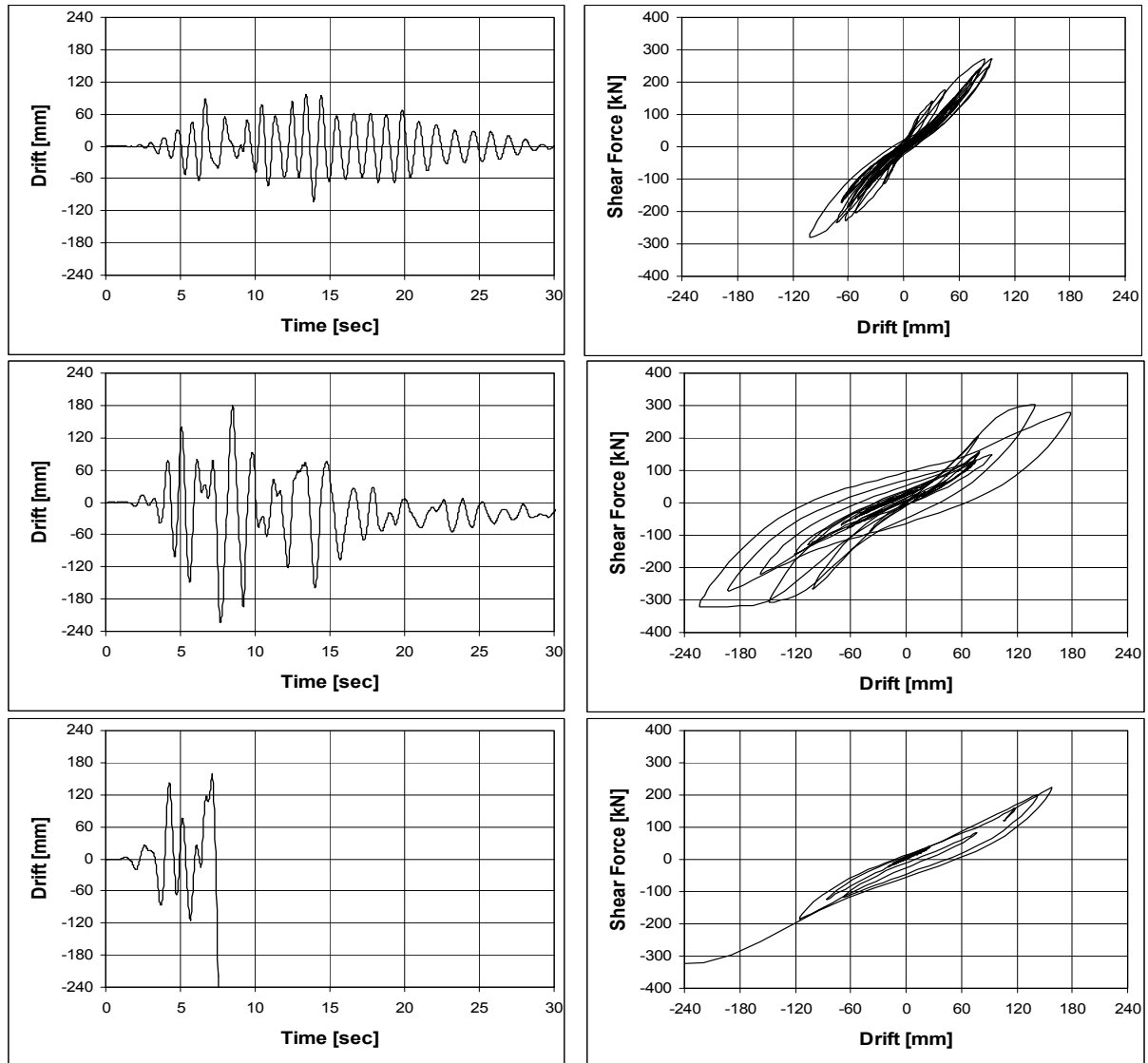


Fig. 15. Displacement time-histories and load-displacement curves measured during the three tests for the intensities $\alpha_g = 0.36$, $\alpha_g = 0.72$ and $\alpha_g = 1.08$.



Fig. 16. View of the precast prototype at the end of the pseudodynamic test.

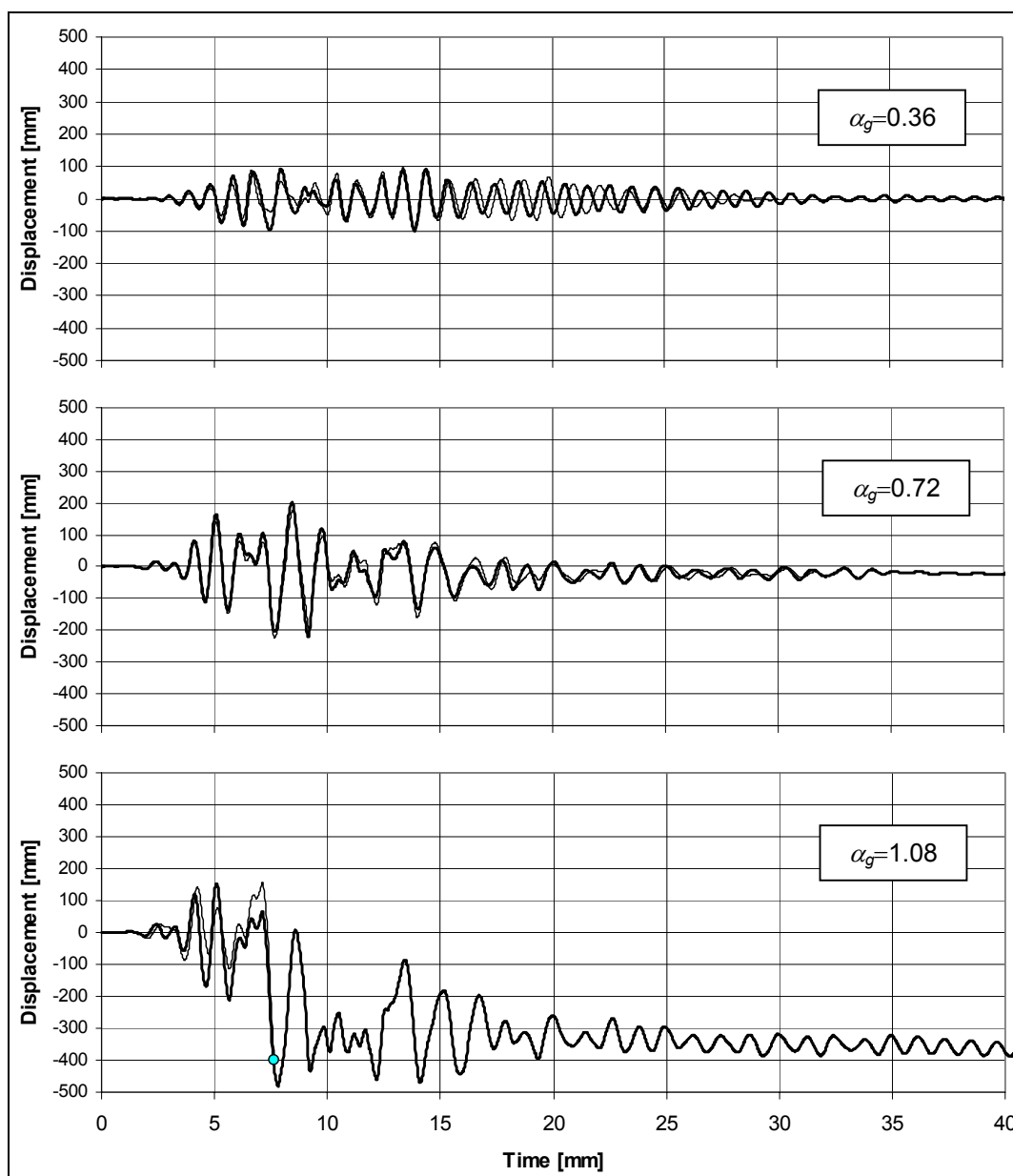


Fig. 17. Displacement time-histories: numerical (thick lines) versus experimental results (thin lines).

The very good correspondence of the computed and experimental responses confirms the reliability of the analytical model and, with it, the results of the preceding statistical analysis. At $\alpha_g=0.36$ level some discrepancies occur around 20 sec and this could indicate the necessity to improve the model for post-cracking small vibrations. At $\alpha_g=0.72$ level the very good coincidence of the two curves indicates the good simulation of the pre- and post-yielding behaviour of the cracked structure. $\alpha_g=1.08$ level the comparison can be made only up to 7.5 sec, time of the test termination. A plausible prediction of the subsequent behaviour seems to be given by the analytical model.

4. CONCLUSIONS

Some general considerations can be advanced. First, the large strength resources of this type of structure against seismic action can be noticed. As reminded in the Introduction, its sensible flexibility and the consequently long natural vibration periods lead to a reduced response. This is foreseen by Eurocode 8, but it is also confirmed by the test results where, for an earthquake of intensity $a_g = 0.36g$ (peak ground acceleration), an elastic response without relevant damages has been shown. For this intensity, which correspond to about the intensity of a 1st category Italian zone for the verification of the ultimate collapse limit, the structure fulfils easily the serviceability conditions of damage limitation. If this intensity is assumed to correspond to the frequent earthquake, we would be in a territory of very high seismicity, where the exceptional earthquake with a return period of 500 years could arrive to $a_g = 0.72g$. But also for this earthquake the experimental response of the prototype showed a very good

elasto-plastic behaviour with little damaging and small residual deformations, indicating that a complete structural restoration was still possible. The precise experimental quantification of the ultimate capacity of the structure has not been given, but also the piece of loading test performed at $a_g = 1.08g$ level allows to think that the theoretical previsions were not so far from the truth, that is that the ultimate strength is about three time larger than what required in Italy for the 1st category zones. And this for a normal dimensioning of the structure, with a reinforcement ratio of the critical zones of the columns equal to about 1.2%. The non seismic conditions (wind pressure, bridge-cranes) could require such reinforcement.

In order to fulfil the limit given by Eurocode 8 to the storey drift, which is defined as the 1 % of the storey height (50 mm in the present case), the intensity of the frequent earthquake should be contained into $a_g = 0.18g$. This value is placed at the ratio $\frac{1}{2}$ with respect to the value assumed in the first loading step.

The conclusion is then that the precast structures of industrial buildings, with their normal dimensions deduced from non seismic conditions, are generally compatible with an Italian seismic zone of 1st category, fulfilling the limit of storey drift under the frequent earthquake, behaving without damages under the exceptional earthquake, maintaining a strength reserve of two time as much with reference to collapse.

ACKNOWLEDGEMENTS

The tests have been performed within the Ecoleader Programme, which is reserved to the European Consortium of Laboratories for Earthquake and Dynamic Experimental Research (JRC – Contract n° HPRI-CT-1999-00059). Particular thanks are given to Mr. Paolo Negro, Mr. Georges Magonette and Mr. Javier Molina who managed the setting up of the instrumentation plant and the execution of the loading tests, ensuring with their high professional ability the perfect accomplishment of the experimentation. Thanks also to Mr. Carlo Bonfanti, who managed the design and the execution of the prototype, for the important contribution of his experience. The research has been led jointly with Prof. Matej Fishinger and his assistants of the Ljubiana University.

REFERENCES

- [01]. CEN-prENV 1998-1, *Eurocode 8: Design of Structures for Earthquake Resistance*, European Committee for Standardization, Brussels, Draft No. 5, November 2002.
- [02]. Biondini, F., Toniolo, G. 2000. Comparative analysis of the seismic response of precast and cast-in-situ r.c. frames. *Studi e Ricerche, Scuola di Specializzazione in Costruzioni in c.a., Politecnico di Milano*, n. 21.
- [03]. Biondini, F., Toniolo, G., and Tsionis, G., *Design Reliability of Cast-in-Situ and Precast Concrete Frames under Recorded Earthquakes. Studies and Researches*, Graduate School for Concrete Structures, Politecnico di Milano, 22, 2001.
- [04]. Biondini, F., and Toniolo, G., *Probabilistic Verification of the Seismic Performance of Precast and Cast-in-situ Reinforced Concrete Frames. Studies and Researches*, Graduate School for Concrete Structures, Politecnico di Milano, 23, 1-17, 2002.
- [05]. Biondini, F., and Toniolo, G., *Probabilistic parameters of the Seismic Performance of Reinforced Concrete Frames. Proc. of the 1st fib Congress*, Paper E-228, Osaka, Japan, October 13-19, 2002.
- [06]. Biondini, F., and Toniolo, G., *Probabilistic Analysis of the Seismic Response of Reinforced Concrete Frames. Proc. of 14° C.T.E. Congress*, Mantova, Italy, November 7-8-9, 2002 (in Italian).
- [07]. Biondini, F., Ferrara, L., Negro, P., and Toniolo, G., *Results of Pseudodynamic test on the Prototype of a Precast R.C. Frame. Proc. of 14° C.T.E. Congress*, Mantova, Italy, November 7-8-9, 2002 (in Italian).
- [08]. Carvalho, E.C., *Prenormative research in support of EC8. European seismic design practice*. Ed. Elnashai, 1995.
- [09]. Park, R., Paulay, T., *Reinforced Concrete Structures*. John Wiley & Sons, 1975.
- [10]. Paulay, T., Priestley, M.J.N., *Seismic design of Reinforced Concrete and Masonry Buildings*. John Wiley & Sons, 1992.
- [11]. *Prefabricated/Industrialised Reinforced Concrete Building Systems (Manual)*, UNDP/UNIDO Project RER/79/015 "Building Construction Under Seismic Conditions in the Balkan Region", 1982.
- [12]. Priestley, M.J.N., Verma, R., Xiao, Y., *Seismic Shear Strength of r.c. Columns*. ASCE Journal of Structural Engineering, 120(8), 2310-2329, 1994.
- [13]. Priestley, M.J.N., *Displacement-based Seismic Assessment of Reinforced Concrete Buildings*. Journal of Earthquake Engineering, 1(1), 157-192, 1997.
- [14]. Qi, X., Pantazopoulou, S.J., *Response of r.c. frame under lateral loads*. ASCE Journal of Structural Engineering, vol. 96, n. 12, 1970.
- [15]. Saisi, A., Toniolo, G., *Precast r.c. columns under cyclic loading: an experimental program oriented to EC8*. Studi e Ricerche, Scuola di Specializzazione in Costruzioni in c.a., Politecnico di Milano, 19, 373-414, 1998.
- [16]. SIMQKE, *A Program for Artificial Ground Motion Generation. User's Manual and Documentation*, NISEE Computer Applications, Department of Civil Engineering, Massachusetts Institute of Technology, 1976.
- [17]. *Strong Motion Collection*, National Geophysical Data Center, Boulder, Colorado, USA, 2000.
- [18]. Takeda, T., Sozen, M.A., Nielsen, N.N., *Reinforced concrete response to simulated earthquakes*. ASCE Journal of the Structural Division, 96(12), 2557-2573, 1970.